Article ID: 1003 - 6326(2003)02 - 0280 - 05

Relationships between deformation mechanisms and initial textures in polycrystalline magnesium alloys AZ31 ①

YANG Ping(杨 平)[1], CUI Feng-e(崔凤娥)[1], BIAN Jian-hua(边建华)[1], G Gottstein[2]
(1. School of Materials Science and Engineering,
University of Science and Technology Beijing, Beijing 100083, China;
2. Institut für Metallkunde und Metallphysik, RWTH Aachen, 52056, Aachen, Germany)

Abstract: Microscopy, X-ray diffractometry and EBSD analysis were applied to inspect the relationships between deformation mechanisms and initial textures in polycrystalline magnesium alloys AZ31. It is found that different deformation mechanisms proceed according to theoretic prediction. Basal slips occur when basal planes of grains are tilted toward normal direction(ND) around transverse direction(TD); prism slips dominate when basal planes are perpendicular to TD. $\{10\bar{1}2\}$ twinning was favored when basal planes are normal to rolling direction(RD) and $\{10\bar{1}1\}$ twinning is analyzed to be related to the basal orientation of grains.

Key words: magnesium alloy; deformation; texture
CLC number: TG 111.7; TG 146.2 **Document code:** A

1 INTRODUCTION

Magnesium is the lightest metallic structural material with high specific strength and is used in automotive, electronics and aerospace field[1, 2]. However, magnesium often shows poor formability at room temperature due to its hexagonal structure with less independent slip systems, which limits its use. Different slip systems have been detected in magnesium such as basal slip of $\{0001\}\langle 11\bar{2}0\rangle$, prism slip of $\{10\bar{1}0\}\langle 11\bar{2}0\rangle$[3, 4] and pyramid slip (including the a-type of $\{hkil\}\langle 11\bar{2}0\rangle$ and the $a+c$ type of $\{hkil\}\langle 11\bar{2}3\rangle$[5, 6]). Besides, different types of twinning may also operate[3, 7, 8]. Therefore deformation mechanisms may be complicated in magnesium. The plasticity of magnesium shows strong anisotropy. Different deformation behaviors and $\sigma-\varepsilon$ curves were observed in single crystal[3, 9, 10]. Poor formability is always related with the strong basal texture $\langle 0001\rangle$ // ND (normal direction). Influence of initial texture on the plasticity in polycrystalline has been investigated and large differences have been found in hot rolled plate AZ31 or pure magnesium at 100 - 200 ℃[11-13]. In order to enhance formability of magnesium, a higher deforming temperature is usually used with two purposes. The first is to activate new slip systems besides basal slip to obtain more than 5 independent slip systems. The possibility lies in that the critical resolve stresses of prism and pyramid slips reduce as temperature increases; while that for basal slip does not change strongly with temperature[14]. The second is to introduce dynamic recrystallization or even super-plasticity[15], which is more accessible in industrial application. This paper aims to inspect the relationship between deformation mechanisms and initial texture in polycrystalline magnesium alloys AZ31 by texture analysis and microstructure observation.

2 EXPERIMENTAL

Materials used were a hot extruded bar with pronounced fiber textures of $\langle 1\bar{1}00\rangle$ and $\langle 11\bar{2}0\rangle$ // extrusion axis and a hot rolled plate with strong $\langle 0001\rangle$ // ND of magnesium alloys AZ31. To eliminate deformed grains samples were annealed at 420 ℃ for 6 h for extruded bar and 500 ℃ for 2 h for hot rolled plate. Although deformed grains disappeared, some grains grew abnormally and the texture intensity decreased in the extruded bar. The grain size of hot-rolled plate was fine (about 25 μm) and homogeneous; while that of extruded bar was 34 μm and inhomogeneous with some grains being larger than 400 μm. Different types of samples were sectioned from annealed samples, named as XZ, ZY and XY for extruded bar and TR and NR for rolled plate, as shown in Fig. 1. The first letter denotes the compression direction during subsequent channel die compression

① **Foundation item:** Project (50171009) supported by the National Natural Science Foundation of China; Project supported by Deutscher Akademischer Austauschdienst and the China Scholarship Council
Received date: 2002 - 08 - 23; **Accepted date:** 2003 - 01 - 08
Correspondence: YANG Ping, Tel: +86-10-62332084; E-mail: yangp@mater.ustb.edu.cn

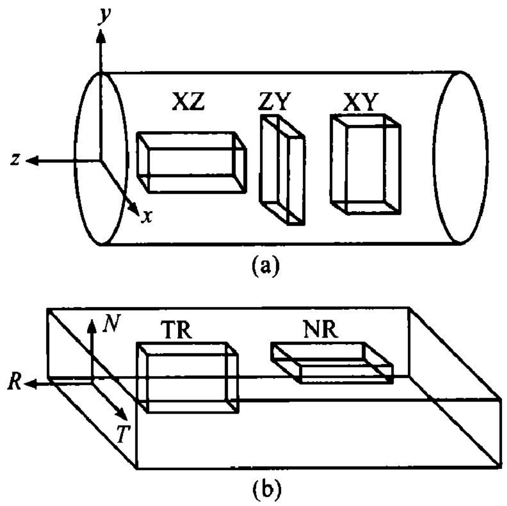

Fig. 1 Preparation of initial samples
(a) —From hot extruded bar; (b) —From hot rolled plate

with respect to the coordinate of extruded bar/plate and the second letter indicates the extension direction, i. e. rolling direction.

Fig. 2 shows the initial textures of samples, in which the Eular angle positions and the Miller-Bravies indices of typical texture components in orientation distribution function (ODF) are also given.

As can be seen from Fig. 2, the basal planes of most grains in the sample TR (also XZ) were nearly perpendicular to TD (transverse direction). The $\langle 1\bar{1}00\rangle$ directions of most grains in the sample ZY were parallel to ND (normal direction), i. e. the normal of basal planes was distributed on the big circle of pole figure. The basal planes of most grains in the sample XY (also NR) were nearly parallel to rolling plane with large scattering around TD. It is noted that there are differences in orientation distributions between samples obtained from extruded bar and from hot-rolled plate. Channel die compression was carried out to realize plane-strain compression at 97 ℃ and 185 ℃ and MoS_2 paste was used as lubricant. The samples were polished in an AC-2 electrolytic solution and were etched in a solution of picric and acetic acid. Six pole figures of $(10\bar{1}0)$, (0002), $(\bar{1}101)$, $(\bar{1}102)$, $(11\bar{2}0)$ and $(\bar{1}103)$ were measured to calculate ODF. For convenience two sections of $\varphi_2 = 0°$ and 30° were used to present texture components. EBSD analysis was performed in an SEM LEO-1450 equipped with HKL Channel 4 system.

3 RESULTS AND ANALYSIS

3.1 Typical microstructures of twins

Fig. 3 shows typical microstructures of twins in different samples. Massive $\{10\bar{1}2\}$ twinning of c-axis tension occurred in sample ZY and twin varieties can be found within grains (as shown in Fig. 3(a)).

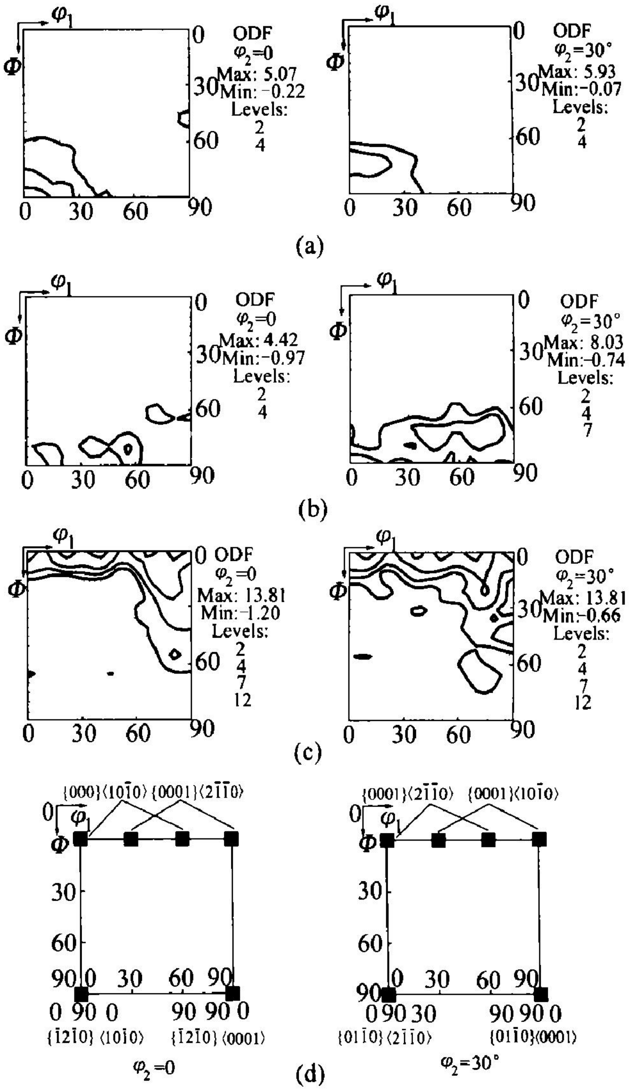

Fig. 2 Initial textures represented in ODF of $\varphi_2 = 0°$ and 30°
(a) —Sample TR; (b) —Sample ZY
(c) —Sample XY; (d) —Typical components in ODF

This is due to the fact that the tension in RD was parallel to c-axis of most grains. The boundaries of this type twin moved very easily. The twins in Fig. 3(b) were thin. It is not clear whether they were of same type with those in Fig. 3(a). The band structure shown in Fig. 3(c) was normally regarded as shear bands and was often found in basal oriented grains because this large grain was nearly basal oriented according to macro-texture (as shown in Fig. 3(d)), i. e. basal plane was parallel to RD (the right direction in Fig. 3(c)). Thus it is impossible to relate the bands with basal slip or basal plane, rather it should be the $\{10\bar{1}1\}$ twinning of c-axis compression. The $\{10\bar{1}1\}$ planes have angles of about ±62° with (0001) plane.

Fig. 4 shows an example of determining orientation and orientation relationship of twin by single orientation measurement in sample XZ deformed by a strain of 25% at 97 ℃. Calculated orientation relationships are also listed. It is seen that the exact

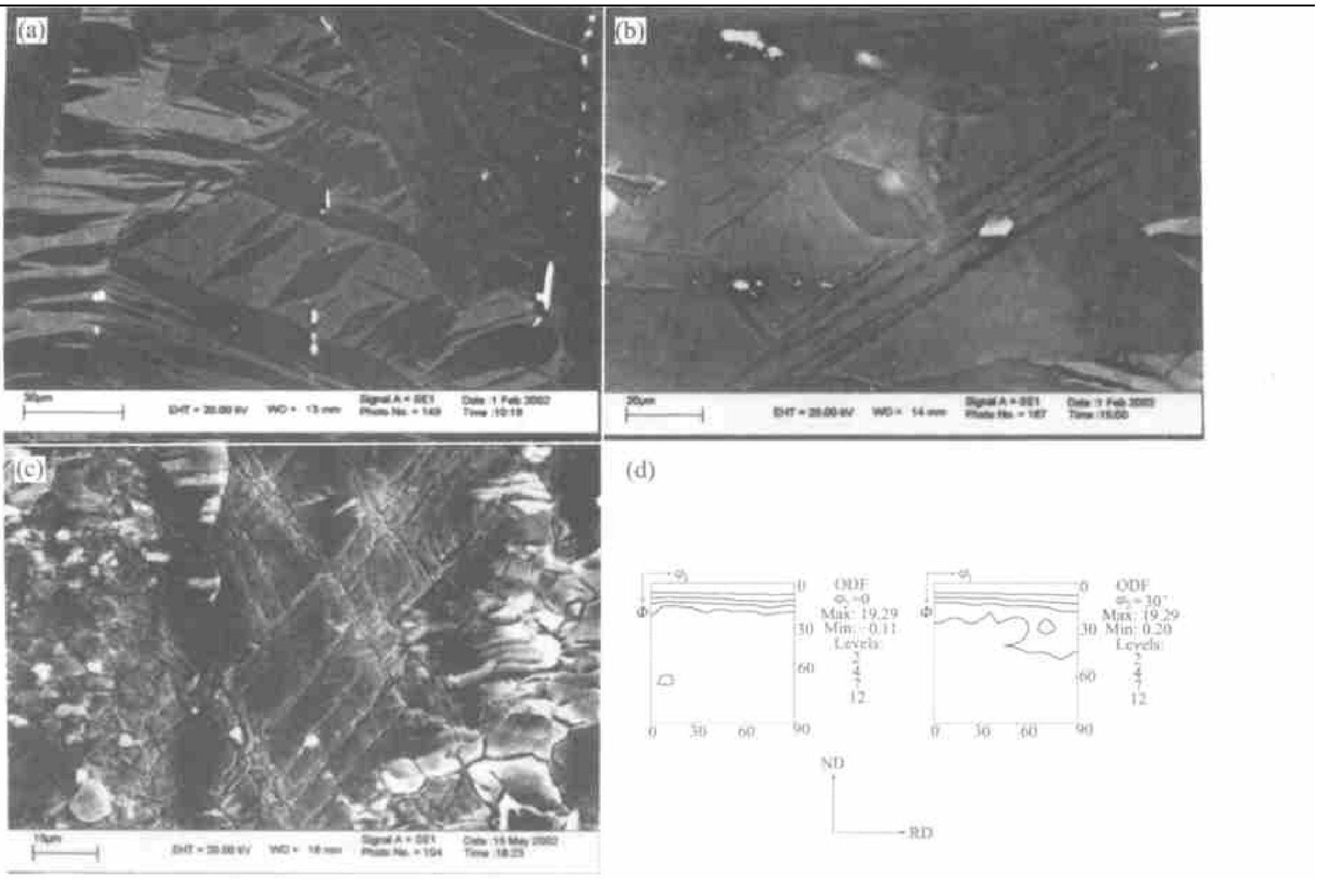

Fig. 3 Typical microstructures of twins
(a) —Sample ZY deformed by strain of 80% at 97 ℃; (b) —Sample XZ deformed by strain of 25% at 185 ℃;
(c) —Sample ZY deformed by strain of 25% at 97 ℃;
(d) —Macro-texture in sample ZY deformed by strain of 25% at 97 ℃

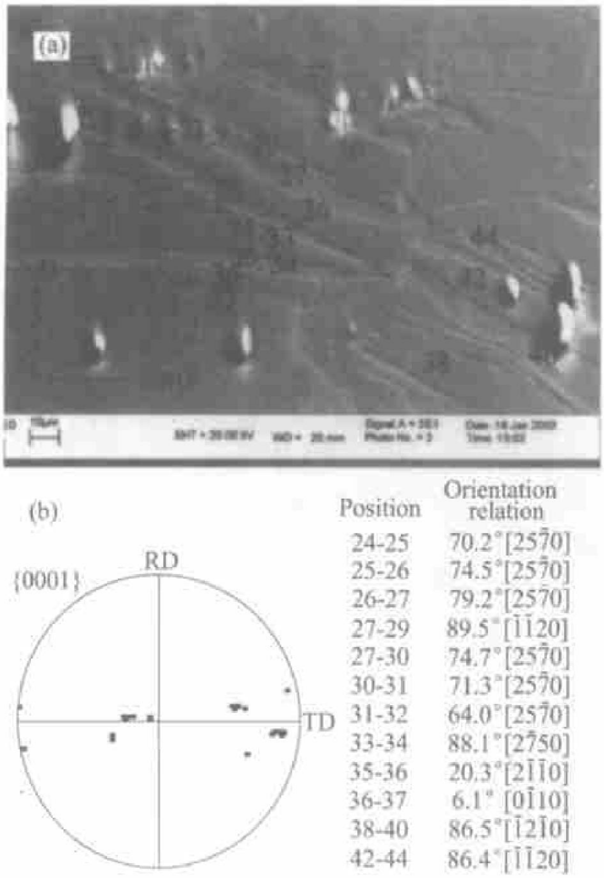

Position	Orientation relation
24-25	70.2°[25$\bar{7}$0]
25-26	74.5°[25$\bar{7}$0]
26-27	79.2°[25$\bar{7}$0]
27-29	89.5°[$\bar{1}\bar{1}$20]
27-30	74.7°[25$\bar{7}$0]
30-31	71.3°[25$\bar{7}$0]
31-32	64.0°[25$\bar{7}$0]
33-34	88.1°[2$\bar{7}$50]
35-36	20.3°[2$\bar{1}\bar{1}$0]
36-37	6.1° [0$\bar{1}$10]
38-40	86.5°[$\bar{1}$2$\bar{1}$0]
42-44	86.4°[$\bar{1}\bar{1}$20]

Fig. 4 Determination of twin relationship by single orientation measurement
(a) —Micrograph; (b) —Orientation

{10$\bar{1}$2} twinning relation of 86.3° ⟨11$\bar{2}$0⟩ was still kept in positions 27 - 29, 38 - 29 and 42 - 44. Other relationships indicate that due to further deformation after the formation of twins scattering from exact twin relationship would occur. Pole figure (as shown in Fig. 4(b)) shows that the matrix of twin was nearly ⟨0001⟩ ∥ TD and twined part was near basal texture orientation (⟨0001⟩ ∥ ND). It has been found in several group orientation measurements that there is no special rule for the scatter of rotation angles, but rotation axis often scattered from ⟨11$\bar{2}$0⟩ to ⟨25$\bar{7}$0⟩, i.e. it rotated preferentially on (0001) plane.

Fig. 5 shows another example of single orientation measurement. The orientation relationships of twins were determined as 63° ⟨11$\bar{2}$0⟩. It may be a {10$\bar{2}$3} ⟨30$\bar{3}$2⟩ type of twin, which is also a twin of c-axis tension[8]. Its twinning shear is close to that of a {10$\bar{1}$2} ⟨10$\bar{1}$1⟩ type of twinning. Here, the twin boundaries are incoherent. However, since this type of twin was very seldom in the sample, it may also be the {10$\bar{1}$2} ⟨10$\bar{1}$1⟩ type twin strongly scattered from exact twin relationship due to deformation.

3.2 Different slip systems

Determination of slip systems can be performed

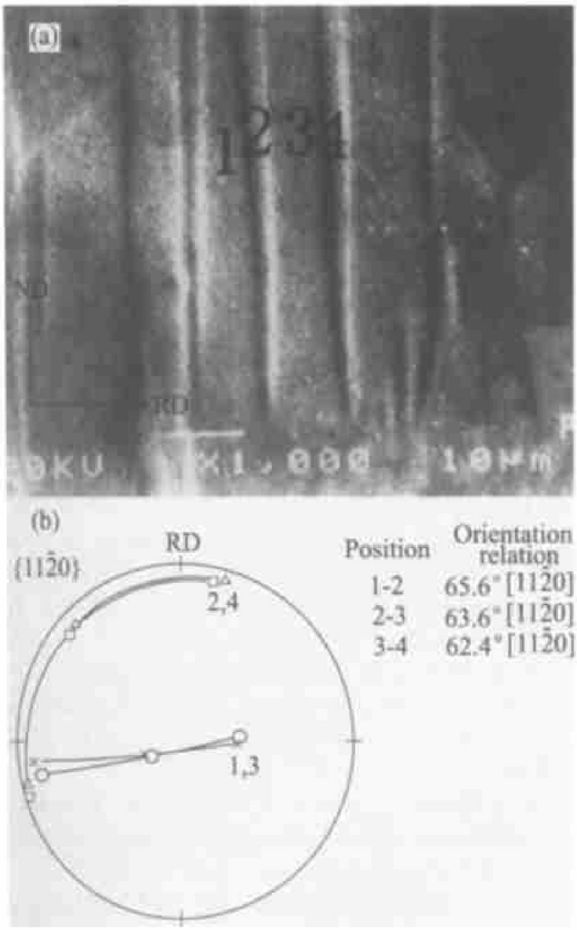

Fig. 5 Determination of twin relationship
(a) —Morphology; (b) —Twin orientation

either by determining Burgers vector under TEM[6, 7] or by analyzing slip traces on sample surfaces[3, 9, 10]. It can also be done by texture analysis. In sample XY the basal planes of many grains in initial samples were parallel to rolling plane with a TD-scattering. This condition favored basal slip, and thus further enhanced basal texture. With the increase of deformation to 80% at 185 ℃, the enhancement of (30, 0, 0) component, i. e. the $\{0001\}\langle 11\bar{2}0\rangle$ component was evident, as shown in Fig. 6. This can be ascribed to the single basal slip because double basal slip will generate (0, 0, 0) component, i. e. the $\{0001\}\langle 10\bar{1}0\rangle$ orientation.

Prism slip can be detected in deformed sample TR (as shown in Fig. 7). The initial texture (0, 90, 30) or $\{01\bar{1}0\}\langle 2\bar{1}\bar{1}0\rangle$ (as shown in Fig. 4 (a)) was unstable. During compression it rotated into the orientation of (0, 90, 0) or $\{\bar{1}2\bar{1}0\}\langle 10\bar{1}0\rangle$ by single prism slip (by comparing Fig. 7 with Fig. 4 (a)) because the single prism slip brought about a rotation of this grain to a large orientation factor until it reached the orientation (0, 90, 0). This orientation (0, 90, 0) was stable. By further compression it remained at this position through double prism slips[4, 5] and its texture intensity became stronger. It is noticed that there existed a clear scattering of orientation (0, 90, 0) around RD (as shown in Fig. 7).

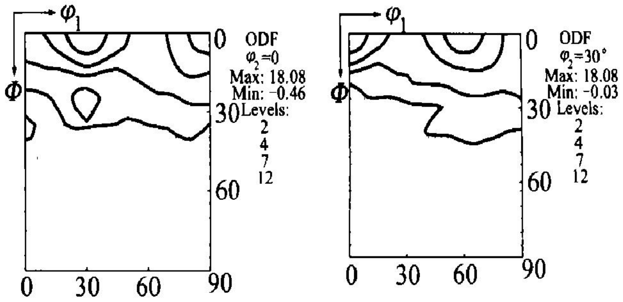

Fig. 6 Texture evolution in sample XY deformed at 185 ℃ with strain of 80%

Because double prism slips can not account for this scattering, simultaneous activation of both double prism slips of $\{10\bar{1}0\}\langle 11\bar{2}0\rangle$ and double basal slips $\{0001\}\langle 11\bar{2}0\rangle$, and perhaps also double pyramid slips of $\{10\bar{1}1\}\langle 11\bar{2}0\rangle$ was postulated to be responsible for this scattering. Referring to Fig. 4(d), it is known that the fiber texture (0, Φ, 0) or $\{hkil\}\langle 10\bar{1}0\rangle$ included all grains whose $\langle 10\bar{1}0\rangle$ is parallel to RD. This means that the two slip directions $\langle 11\bar{2}0\rangle$ on a basal plane and two slip directions $\langle 11\bar{2}0\rangle$ on two prism or two pyramid planes have similar orientation factors, therefore, double basal slip, double prism slip and/or double pyramid slips would operate simultaneously. In addition, as the rotation of a grain caused by basal slips is opposite to that caused by prism slips, there will be a balance between them, i. e. more independent slip systems were active in the presence of this scattering.

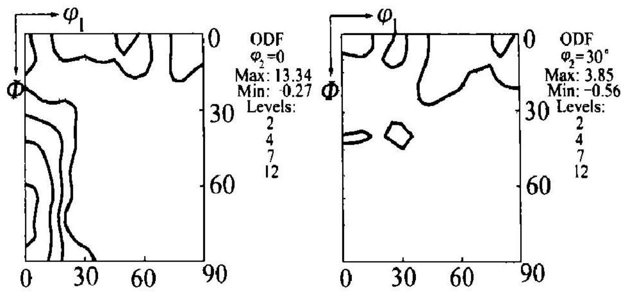

Fig. 7 Texture in sample TR deformed at 185 ℃ with strain of 60%

5 CONCLUSIONS

EBSD analysis and texture analysis indicate that there is a clear relationship between deformation mechanisms and initial textures in polycrystalline magnesium alloys AZ31 and this relationship is similar to that in single crystal of magnesium. Different deformation mechanisms proceeded according to theoretic prediction. Basal slip occurred mainly when basal planes were tilted toward ND around TD; prism slip dominated when basal planes were perpendicular to TD. $\{10\bar{1}2\}$ twinning was favored when basal planes were normal to RD and $\{10\bar{1}1\}$ twinning was favored when grains were in basal orientation. The scattering of (0, 90, 0) around RD was ascribed to the simultaneous operation of double prism and basal slips which provided more independent slip systems and formability.

REFERENCES

[1] Sebastian W, Droeder K, Schumann S. Properties and processing of magnesium wrought products for automotive application [A]. Proc of Magnesium Alloys and their Applications [C]. Munich Germany: DGM inter congress, 2000. 602 - 608.

[2] Landkof B. Magnesium applications in aerospace and electronic industries [A]. Proc of Magnesium Alloys and their Applications [C]. Munich Germany: DGM inter congress, 2000. 168 - 172.

[3] Kelley E W, Hosford W F Jr. Plane-strain compression of magnesium and magnesium alloy crystals [J]. Trans AIME, 1968, 242: 5 - 13.

[4] Ward F P, Mote J, Dorn J E. On the thermally activated mechanism of prismatic slip in magnesium single crystals [J]. Trans AIME, 1961, 221: 1148 - 1154.

[5] Obara T, Yoshinga H, Morozumi S. $\{\bar{1}\ \bar{1}22\}\langle\bar{1}123\rangle$ slip system in magnesium [J]. Acta Metall, 1973, 21: 845 - 853.

[6] Agnew S R, Yoo M H, Horton J A. Texture analysis as a tool for wrought magnesium alloy development [A]. Proc of Magnesium Alloys and their Applications [C]. Munich Germany: DGM inter congress, 2000. 119 - 124.

[7] Klimanek P, Poetzsch A. Microstructure evolution under compressive plastic deformation of magnesium at different temperatures and strain rates [J]. Mater Sci and Eng, 2002, A324: 145 - 150.

[8] Yoo M H. Slip, twinning, and fracture in hexagonal close-packed metals [J]. Metall trans, 1981, 12A: 409 - 418.

[9] Kelley E W, Hosford W F Jr. The deformation characteristics of textured magnesium [J]. Trans AIME, 1968, 242: 654 - 660.

[10] Wonsiewicz B C, Backofen W A. Plasticity of magnesium crystals [J]. Trans AIME, 1967, 239: 1422 - 1431.

[11] Gehrmann R, Gottstein G. Texture and microstructure development during plastic deformation of magnesium [A]. Proc of 12th Inter Conf on Textures of Mater [C]. Montreal, Canada, 1999. 665 - 670.

[12] Gehrmann R, Frommert M M, Gottstein G. Influence of texture on deformation behavior of magnesium alloy AZ31 [A]. Proc of Magnesium Alloys and their Applications [C]. Munich Germany: DGM Inter Congress, 2000. 143 - 148.

[13] Yi S, Brokmeier H-G, Bolmaro. Texture development and texture influence on the mechanical properties of the Mg-alloy AZ31 [J]. Materials Sci Forum, 2002, 408 - 412: 1067 - 1072.

[14] Ion S E, Humphreys F J, White S H. Dynamic recrystallization and the development of microstructure during the high temperature deformation of magnesium [J]. Acta Metall, 1982, 30: 1909 - 1919.

[15] Tan J C, Tan M J. Superplasticity and grain boundary sliding characteristics in two stage deformation of Mg-3Al-1Zn alloy sheet [J]. Mater Sci & Eng, 2003, A339: 81 - 89.

(Edited by YANG Bing)